

**SCHOOL OF MATERIALS AND MINERAL RESOURCES ENGINEERING
UNIVERSITI SAINS MALAYSIA**

CORROSION BEHAVIOR OF QUENCHED SAC305 SOLDERS

By

NOR SYAFIQAH BINTI MUHAMAD

Supervisor: Assoc. Prof. Dr. Ahmad Azmin bin Mohamad

Dissertation submitted in partial fulfillment
of the requirements for the degree of Bachelor of Engineering with Honours
(Materials Engineering)

Universiti Sains Malaysia

JUNE 2018

DECLARATION

I hereby declare that I have conducted, completed the research work and written the dissertation entitled “**Corrosion Behavior of Quenched SAC305 Solders**”. I also declare that it has not been previously submitted for the award of any degree or diploma or another similar title of this for any other examining body or university.

Name of Student: Nor Syafiqah Binti Muhamad

Signature:

Date: 25 June 2018

Witnessed by

Supervisor: Assoc. Prof. Dr. Ahmad Azmin bin Mohamad

Signature:

Date: 25 June 2018

ACKNOWLEDGEMENTS

First of all, Alhamdulillah and all praise to God, the Almighty for His blessing throughout my final year project to complete this project successfully.

I would like to deliver my deepest appreciation to my supervisor Assoc. Prof. Dr. Ahmad Azmin bin Mohamad that helped and gives guidance to me throughout this project in completing this thesis. I am extremely thankful and indebted to him for sharing expertise, inspiration, valuable guidance and encouragement extended to me. It is truly an honor to be assigned under his supervision for this final project.

Next, I would like to express special thanks to the technician, academic and administrative staffs of School of Materials and Mineral Resources Engineering (SMMRE), for helping me in the utilization of equipment and recommendations on my final year project. They are kept in teaching and assisting me when dealing with the machines and equipment. I also like to extend my thanks and gratitude to my senior, Ibrahim Ahmad and Nor Azmira Salleh for their tips and useful advice that has given to me throughout the duration of my project.

Last but not least, special thanks to all my family members and my course-mates in USM for their encouragement, moral and financial support in all the good and hard times.

TABLE CONTENTS

Contents	page
DECLARATION	ii
ACKNOWLEDGEMENTS	iii
TABLE OF CONTENTS	iv
LIST OF TABLES	vii
LIST OF FIGURES	viii
LIST OF ABBREVIATIONS	xiv
LIST OF SYMBOLS	xv
ABSTRAK	xvi
ABSTRACT	xvii
CHAPTER 1: INTRODUCTION	1
1.1 Background	1
1.2 Problem Statement	3
1.3 Objectives	4
1.4 Scope of Work	4
CHAPTER 2: LITERATURE REVIEW	5
2.1 Introduction	5
2.2 SAC305 solder alloy	5
2.3 Cooling methods	7
2.4 Effect of reflow time	10
2.5 Effect of cooling rate	13

2.6	Corrosion characterization of SAC305 solders	18
2.7	Morphology and elemental analysis	26
CHAPTER 3: METHODOLOGY		30
3.1	Introduction	30
3.2	Flow chart	30
3.3	Material and equipment	32
3.4	Sample preparation	33
3.5	Electrochemical characterization	37
	3.5.1 Open circuit potential	37
	3.5.2 Potentiodynamic polarization	38
3.6	Characterization of SAC305 solder of different cooling methods	40
CHAPTER 4: RESULTS AND DISCUSSIONS		41
4.1	Introduction	41
4.2	Materials characterization of the SAC305 solders	42
	4.2.1 Effect on phases	42
	4.2.2 Effect on the microstructure and elemental analysis at surface	45
	4.2.3 Effect on the microstructure and elemental analysis at cross-section	51
4.3	Electrochemical characterization of SAC305 solders	57
	4.3.1 Open circuit potential	57
	4.3.2 Potentiodynamic polarization	59
4.4	Corrosion characterization of SAC305 solders	63
	4.4.1 Effect on the structural after open circuit potential	63

4.4.2 Effect on the structural after potentiodynamic polarization	66
4.4.3 Effect on the morphological and elemental analysis after open circuit potential	66
4.4.4 Effect on the morphological and elemental analysis after potentiodynamic polarization	73
CHAPTER 5: CONCLUSION AND FUTURE WORKS	80
5.1 Conclusion	80
5.2 Recommendation for Future Works	81
REFERENCES	82
APPENDICES	88

LIST OF TABLES

	Page
Table 2.1: The melting temperature of several lead-free solder alloy (Nomura et al. 2015)	7
Table 2.2 Potentiodynamic polarization parameters for SA, SAC 305 and SAC 105 solder alloys in 3.5 wt% NaCl solution (Fayeka, Haseeb and Fazal, 2017)	25
Table 3.1: Materials and equipment	32
Table 4.1: Potentiodynamic polarization parameter of different cooling methods of SAC305 solder alloy in 3.5 wt% NaCl solution	62

LIST OF FIGURES

	Page
Figure 2.1:	General soldering profile (Ting et al. 2015) 8
Figure 2.2:	The thermal profiles of the Sn-3.5Ag/Cu joint during reflow and cooling in three different media (Deng et al. 2003) 10
Figure 2.3:	XRD analysis of SAC305/Cu at different reflow temperature (a) 230, (b) 240, (c) 250, and (d) 260°C for 30 s (Lee et al. 2013) 11
Figure 2.4:	SEM micrographs of solder joints showing the IMC layers after (a) reflowing for 20 s and (b) reflowing for 600 s (Tu et al. 1997) 12
Figure 2.5:	XRD pattern of SAC305 solder alloy at different cooling method (Wei & Wang 2012) 13
Figure 2.6:	(a) The microstructure of SnAgCu solder (Sun and Zhang, 2015), (b) air cooled and (c) water cooled (Ji et al. 2014) 15
Figure 2.7:	The microstructure of solder joints cooling in water, cooling in air cooling in a furnace for (a,c,e) (Hu et al. 2016) and (b,d,f) (Deng et al. 2003), (Lee and Huang, 2015) 16
Figure 2.8:	SEM images of SAC305 solder joints: (a) quenched in water, (b) cooled in air, (c) cooled in a furnace, (d) Variation of the thickness of the interfacial Cu ₆ Sn ₅ IMC layer (Yang and Zhang, 2015) 18
Figure 2.9:	Open circuit potential (OCP) of lead-free solders (Martin et al. 2015) 20

Figure 2.10:	Potentiodynamic polarization curves of SAC305 solders at different cooling methods in 3.5 wt% NaCl solution (Wang et al. 2012)	21
Figure 2.11:	XRD pattern from corrosion products of SAC305 solders after anodic polarization at +500 Mv /SCE for 1800 s in 3.5 wt% NaCl solution at 25 °C (Wang et al. 2012)	22
Figure 2.12:	Potentiodynamic polarization curves of SA, SAC 305 and SAC 105 solder alloys in 3.5 wt% NaCl solution (Fayeka et al. 2017)	23
Figure 2.13:	X-ray diffraction pattern of SAC105 and SAC305 after polarization (Fayeka, Haseeb, and Fazal, 2017)	24
Figure 2.14:	Schematic diagram with FESEM images of the as-reflowed SAC305/Cu, with (a) and (b) are captured before the polarization test, whereas (c) and (d) are observed after the polarization test in 6 M KOH solution (Liew et al. 2012)	27
Figure 2.15:	SEM images and EDX analysis of SAC305 solders polarized to +1,500 mV/SCE in 3.5 wt% NaCl solution (a,b) commercial SAC305 solder, (c,d) air-cooled solder and (e,f) furnace-cooled solder (Wang et al. 2012) (Wang, Wang and Ke, 2014b)	29
Figure 3.1:	Flow chart for a methodology	31
Figure 3.2:	The preparations of the reflowing of SAC305 solder paste on copper substrate	33
Figure 3.3:	SAC305 solder after reflow in furnace cooled	33

Figure 3.4:	Solder wetting process (a) SAC305 solder on the Cu substrate, (b) liquid solder spreading over the Cu substrate, (c) Cu diffuse in the liquid solder, and (d) Cu reacting with the liquid solder to form an intermetallic compound layer	34
Figure 3.5:	Cross-section of reflowed SAC305 solder in furnace cooled	35
Figure 3.6:	Cross-section of SAC305 solder after connected with electrical wire for OCP and potentiodynamic polarization test	36
Figure 3.7:	The mounted SAC305 solder (a) that have been polished (b) preparation for OCP and potentiodynamic polarization (c) Schematic diagram of mounted SAC305 solder	37
Figure 3.8:	(a) Experimental setup for OCP test and (b) schematic diagram of the setup for the OCP test of SAC305 solder	38
Figure 3.9:	(a) Experiment setup of Potentiodynamic polarization test and (b) schematic diagram of the setup for the potentiodynamic polarization test of SAC305 solder	39
Figure 4.1:	XRD pattern of SAC305 solder at different cooling methods (a) furnace cooled and (b) ice quenched	43
Figure 4.2:	XRD pattern of SAC305 solder at different position and intensities at (a) 42-45°, (b) 49-52° and (c) 73-75°	44
Figure 4.3:	FESEM image of SAC305 solder cooled by furnace at surface in different magnification (a) 300X, (b) 500X, (c) 1.0kX and (d) 2.0kX	46
Figure 4.4:	EDX analysis of SAC305 solder cooled by furnace at surface	47

Figure 4.5:	FESEM image of SAC305 solder cooled by ice at surface in different magnification (a) 300X, (b) 500X, (c) 1.0kX and (d) 2.0kX	48
Figure 4.6:	EDX analysis of SAC305 solder cooled by ice at the surface	49
Figure 4.7:	Comparison of FESEM image of SAC305 solder (a) furnace cooled and (b) ice quenched at the surface	50
Figure 4.8:	Cross-section of furnace cooled microstructure of SAC305 solder at different magnification (a) 500X, (b) 1kX, (c) 2.0kX and (d) 2.5kX	52
Figure 4.9:	EDX analysis of SAC305 solder cooled by furnace at cross-section	53
Figure 4.10:	Cross-section of ice quenched microstructure of SAC305 solder at different magnification (a) 500X, (b) 1kX, (c) 2.0kX and (d) 2.5kX	54
Figure 4.11:	EDX analysis of SAC305 solder cooled by ice at cross-section	55
Figure 4.12:	Cross-section microstructures of SAC305 solder by (a) furnace cooled and (b) ice quenched	57
Figure 4.13:	OCP profile for furnace cooled and ice quenched of SAC305 solder in 3.5 wt% NaCl solution	59
Figure 4.14:	Potentiodynamic polarization curves of furnace cooled and ice quenched in 3.5 wt% NaCl solution	62
Figure 4.15:	XRD pattern of SAC305 solder at different cooling methods (a) furnace cooled and (b) ice quenched after OCP	64

Figure 4.16:	XRD pattern of SAC305 solder at different cooling methods (a) furnace cooled and (b) ice quenched after potentiodynamic polarization	66
Figure 4.17:	FESEM image of SAC305 solder of furnace cooled at different magnification after OCP at different magnification (a) 300X, (b) 500X, (c) 1.0kX and (d) 2.0kX	67
Figure 4.18:	EDX analysis of SAC305 solder cooled by furnace after OCP	68
Figure 4.19:	FESEM image of SAC305 solder of ice quenched at different magnification after OCP test at different magnification (a) 300X, (b) 500X, (c) 1.0kX and (d) 2.0kX	69
Figure 4.20:	EDX analysis of SAC305 solder cooled by ice after OCP	70
Figure 4.21:	FESEM image of SAC305 solder in (a) furnace cooled and (b) ice quenched after OCP	71
Figure 4.22:	Schematic mechanism of corrosion product of SAC305 solder in (a) furnace cooled and (b) ice quenched after OCP	72
Figure 4.23:	FESEM image of SAC305 solder of furnace cooled after polarization test at different magnification (a) 300X, (b) 500X, (c) 1.0kX and (d) 2.0kX	74
Figure 4.24:	EDX analysis of SAC305 solder cooled by furnace after polarization	75
Figure 4.25:	FESEM image of SAC305 solder of ice quenched after polarization test at different magnification (a) 300X, (b) 500X, (c) 1.0kX and (d) 2.0kX	76

Figure 4.26:	EDX analysis of SAC305 solder cooled by ice after polarization	77
Figure 4.27:	FESEM image of SAC305 solder of (a) furnace cooled and (b) ice quenched after polarization test	78
Figure 4.28:	Schematic mechanism of corrosion product of SAC305 solder in (a) furnace cooled and (b) ice quenched after potentiodynamic polarization	79

LIST OF ABBREVIATIONS

FESEM	Field Emission Scanning Electron Microscopy
XRD	X-ray Diffraction
EDX	Energy Dispersive X-ray
IMC	Intermetallic Compound
OCP	Open Circuit Potential
RE	Reference Electrode
WE	Working Electrode
CE	Counter Electrode
ICDD	International Centre of Diffraction Data
E_{corr}	Corrosion Potential
E_{pass}	Passivation Potential
i_{cc}	Critical Current Density
i_{pass}	Passivation Current
i_{corr}	Corrosion Current Density

LIST OF SYMBOLS

μm	micrometer
mm	millimeter
cm	centimeter
NaCl	Sodium chloride
$^{\circ}\text{C}/\text{s}$	Degree Celsius per second
mV	millivolt
mV/s	millivolt per second
mA/cm^2	miliampere per centimetre square
$^{\circ}\text{C}$	Degree Celsius
%	Percentage
s	Second

KELAKUAN KAKISAN OLEH PENYEJUKAN PATERI LOGAM SAC305

ABSTRAK

Kesan kelakuan kakisan kepada penyejukan pateri logam SAC305 dengan kaedah seperti penyejukan relau dan pelindapkejutan ais telah disiasat. Fasa tipikal yang terdapat dalam pateri logam SAC305 dengan kaedah penyejukan yang berbeza adalah β -Sn, Ag_3Sn dan Cu_6Sn_5 . Mikrostruktur penyejukan relau lebih kasar daripada mikrostruktur pelindapkejutan ais. Ketebalan lapisan sebatian antara logam (IMC) lebih tebal ($4.558 \mu m$) untuk penyejukan relau dan nipis ($1.532 \mu m$) untuk pelindapkejutan ais. Penyejuk relau mempunyai lebih banyak masa untuk fasa Sn dan pertumbuhan eutektik berbanding dengan pelindapkejutan ais yang mempunyai masa yang terhad. Kelakuan pengaratan bagi kaedah penyejukan yang berbeza telah disiasat dalam larutan 3.5 wt% NaCl oleh potensi litar terbuka dan polarisasi potentiodynamik. Berdasarkan keluk polarisasi potentiodynamik, pelindapkejutan ais menunjukkan liputan pasif yang lebih besar dan ketumpatan arus pasifasi yang lebih rendah yang menunjukkan perlindungan lapisan pasif lebih stabil. Fasa, morfologi dan analisis unsur digunakan untuk mencirikan sampel pateri logam SAC305 pada kadar penyejukan yang berlainan. Di samping itu, analisis mikrostruktural dan elemen mendedahkan kehadiran oksida pada permukaan sampel yang berkarat. Saiz butiran produk kakisan dalam penyejukan relau lebih besar dan oksida yang terkandung dalam bentuk plat yang besar berbanding dengan pelindapkejutan ais yang mempunyai bentuk plat yang seragam dan kecil. Keputusan menunjukkan bahawa sampel pelindapkejutan ais mempamerkan ketahanan karat yang lebih baik daripada sampel penyejukan relau disebabkan oleh lapisan produk karat yang padat dan dapat melindungi permukaan pateri logam SAC305.

CORROSION BEHAVIOR OF QUENCHED SAC305 SOLDER ALLOY

ABSTRACT

The effect of corrosion behavior of quenched SAC305 solder alloy with different cooling methods such as furnace cooled and ice quenched were investigated. Typical phases present in SAC305 solder with different cooling methods were β -Sn, Ag_3Sn and Cu_6Sn_5 . The microstructure of furnace cooled was coarser than microstructure of ice quenched. The thickness of IMC layer was thicker (4.558 μm) for furnace cooled and thinner (1.532 μm) for ice quenched. The growth of Sn and eutectic phases were longer for furnace cooled and has limited time for ice quenched. The corrosion behavior of different cooling methods was investigated in 3.5 wt% NaCl solution by open circuit potential (OCP) and potentiodynamic polarization. Based on potentiodynamic polarization curve, ice quenching exhibit larger passivation range and lower passivation current density indicates more stable and protective passive layer. Phases, morphologies and elemental analysis were used to characterize the sample of SAC305 solder at different cooling rate. In addition, the microstructural and elemental analysis revealed the presence of oxide on the surface of the corroded sample. The grain size of corrosion product in furnace cooled sample was larger and the oxide form was large plate-like shape as compared to ice quenched sample that has a uniform and small plate-like shape. Results showed that ice quenched sample exhibits better corrosion resistance than furnace cooled sample due to compact corrosion product layer that can protect the surface of the SAC305 solder alloy.

CHAPTER 1

INTRODUCTION

1.1 Background

Worldwide research has been undertaken to find lead-free substitutes for lead-containing solders due to high toxicity of lead and growing concern about human health and environment. The Sn-Ag, Sn-Ag-Cu, Sn-Cu solders are promising lead-free solders alloy to replace lead solders (Yu et al. 2000). Hence, Shiv prasad and Padhy, (2015) stated that Sn₃Ag_{0.5}Cu (SAC305) was observed to have better wettability, solderability and melting temperature also lower which is 217 °C compared with the Sn-Ag (221°C). However, SAC305 need to meet the technical requirement such as corrosion resistance, wettability, thermal and electrical conductivity, melting point and also low cost (Siewert et al. 2003).

The formation of excessive growth of intermetallic compound (IMC) in a solder joint can be harmful due to the brittleness and more susceptible to crack that can often cause embrittlement to the solder joints. However, the IMC is an indication of chemical bonding at the substrate or at the solder interface. Then, small amounts of intermetallic compounds can be contributed to good bond hardness and strength (Deghaid Pereira et al. 2013). In addition, lower thickness of IMC can even produce some improvements in the mechanical and thermal properties of solder joints. A layer of Cu₃Sn was formed between Cu₆Sn₅ and the Cu substrate when the solder joint is aged at high temperature or a long time. Generally, the IMCs layer will affect the reliability and microstructure of the solder joint when the thickness of IMCs higher (Hu et al. 2013).

SnAgCu was used in the electronic industries due to its lower toxicity and as the replacement of Sn-Pb. Corrosion in the solder joints needs to be taken care to avoid the serious problem for a long time of the solder joint. The effect of corrosion of Sn-Ag-Cu can observe due to exposing of moisture absorption, humid condition and brackish atmosphere in the application. This condition should be avoided in order to have long-lasting electronic devices. Currently, sodium chloride (NaCl) electrolyte was used in Sn-Ag-Cu to investigated the effect of corrosion behavior of the sample in seawater condition (Rosalbino et al. 2009).

The potentiodynamic polarization test was used to study the effect of corrosion behavior of these lead-free solders to the solder joints. The investigation on the corrosion resistance of Sn-Pb and several lead-free solders in 3.5 wt% of NaCl electrolyte through potentiodynamic polarization was studied. The results showed that lead-free solders have better corrosion resistance compared to the Sn-Pb solders. This phenomenon occurred because of the lower passivation current density and lower corrosion current density obtained by the lead-free solder after the passivation film breakdown. More stable passivation film on the surface can obtained due to breakdown of current density (Li et al. 2008).

1.2 Problem Statement

In the solder reflow process, different type of microstructure in the SAC solder could be obtained when applied different cooling rate, and this will affect to the reliability of the solder joint. Improper cooling rate coarsen the phases in solder matrix, thereby degrading the mechanical properties of the solder. For SAC solder joint, the intermetallic compounds (IMCs) exist in form of small particles, fibers or large plates depending on the cooling rate.

Different cooling method such as furnace cooling, air cooling and water cooling had been studied. However, the effect of extreme cooling (ice quenching) methods of SAC305 solder on corrosion has not been explore in previous research. The effect from the changes of microstructure and phases will influence the properties of the solder.

The cooling rate in the solidification stage is importance in order to receive a good solder joint. Different microstructure of solder could obtain when solder joint is cooled at a different rate. When the cooling rate of the solder joint was not even, then non uniform microstructure of solder could be obtained which would affect the corrosion behavior of solder.

1.3 Objectives

The objectives of this research are:

- i. To characterize the structural, morphology, and elemental analysis of SAC305 solder after furnace cooled and ice quenched.
- ii. To investigate the effect of quenching on corrosion behaviour by analyse the result of OCP and Tafel plot.
- iii. To study phase and microstructure of ice quenched in SAC305 solder prior to corrosion test.

1.4 Scope of Work

Overall, this research work was categorized into five chapters. Chapter one explained generally about the introduction of the research including the problem statement, objectives and scope of the research. Meanwhile, concept, theory and literature review regarding the effect of the different cooling method on SAC305 solder and also its microstructure by corrosion test in Chapter two. The syntheses of corrosion methods were also elaborated in this chapter. Chapter three enlightened on the methodology that explains how the laboratory investigation will be held while performing the experiment. The experimental details and characterization approaches were explained respectively. Then, Chapter four focused on the results and discussion of this project. Finally, the conclusion of the research work was stated in Chapter five.

CHAPTER 2

LITERATURE REVIEW

2.1 Introduction

In this chapter, the effect of the different cooling methods on SAC305 solder alloy, the growth mechanism of intermetallic compounds (IMC) of solder alloy and also the corrosion behavior of quenched SAC305 solder alloy was discussed. X-ray Diffraction analysis (XRD), Scanning Electron Microscopy (SEM) and Energy Dispersive X-ray (EDX) were used to obtain information about the phases, microstructure and elemental analysis of solder alloys before and after the electrochemical characterization. Then, briefly describe the characterization technique used in this study, which is open circuit potential and potentiodynamic polarization.

2.2 SAC305 solder alloy

In the electronics industry, lead-solder can lead to pollute our environment and give effect to the human health due to disposal of electronic assemblies like cell phones and electronic toy. Its inherent toxicity considered as hazardous to the environment. Kotadia et al. (2014) stated that the least expensive elements on Earth is Pb and its replacement need high cost. However, the main concern is based on the reliability, and whether the new lead-free solder alloys can have better performance level of their used. In order to enhance the impact reliability of electronics, Yu et al. (2014) stated that the structure and the composition of solder joints in electronic packages should be designed in good ways.

Cheng et al. (2017) stated that the main requirements for solder alloy refer to the low melting point, high wettability, low cost, and availability. The melting point should be low enough as possible in order to avoid thermal damage to the soldered sample and high enough for the solder joint to resist the operating temperatures applied. Lead-free solder was used in the manufacturers of electronic system and component to lower the cost and increase the wettability unless it has demonstrated better properties. The good wettability is the reaction of bond between the solder and the base metal have formed only when the solder wets the base metal properly (Wu et al. 2004).

A good wettability and mechanical performance of the solder joint was refer to SAC solder because it had been proposed as the most promising substitute for Pb-containing solders (Chen et al. 2002). On the other hand, SAC305 solder had been concerned to have such coarse and brittle intermetallic compound (IMC) that will reduce the mechanical and electronic reliability when the cooling rate is lower. This IMCs grow will affect the performance of the microelectronic device. IMCs such as Cu_6Sn_5 and Ag_3Sn solder play an important role in solder joints and in order to determine strength to the surrounding solder matrix. Therefore, the most suitable for present PCBs components are Sn-Ag-Cu (Jung et al. 2018). Table 2.1 showed the melting temperature of different lead-free solder alloy.

Table 2.1: The melting temperature of several lead-free solder alloy (Nomura et al. 2015)

Solder	Composition	Melting temperature (°C)	
		Solidus	Liquidus
SAC 105	Sn-1.0Ag-0.5Cu	217	227
SAC305	Sn-3.0Ag-0.5Cu	217	220
SAC405	Sn-4.0Ag-0.5Cu	217	229
SACBN308	Sn-3.0Ag-0.8Cu-3Bi-Ni	205	215

In addition, corrosion behavior of Sn–Pb solder joints has been a concern because the oxide formed on the tin-lead alloy is relatively stable. The difference in galvanic potentials of lead and tin is small, therefore the less effect on the corrosion behavior in moisture condition or environment. On the other hand, the presence of intermetallic compounds (IMCs) and their effects on the corrosion behavior of lead-free solder alloy have more attention (Freitas et al. 2014). The presence of three phases of fine Ag_3Sn , Cu_6Sn_5 IMCs and β -Sn on their contributions to the joint of ternary SAC alloys have been investigated based on different type of cooling rate (Song and Lee, 2006).

2.3 Cooling methods

In this section, the effect of cooling methods has influenced the phases, microstructure, composition and corrosion behavior of SAC305 solder. All these were discussed and reviewed. There are several types of cooling method that reviewed in this section, which are furnace cooling, air cooling, and water quenching. Usually, different

cooling methods will have a different cooling rate of the solder. The corrosion behavior of these methods was studied based on the electrochemical characterization.

Figure 2.1 stated, the solder joint is heated to a temperature of 50 to 100 °C below the liquidus temperature during preheating and held at that temperature for a while. Next, the soldering temperature is increase to the peak temperature which is 30 to 50 °C above the solder liquidus temperature. To reduce the temperature, the joint is then soaked in this temperature for a couple of minutes. Lastly, it is cooled down to room temperature and solidified to form a soldered joint. The selection temperature for SAC solder joining is usually around 250 °C as the liquidus temperature of SAC solders is approximately around 217 °C (Ting et al. 2015).

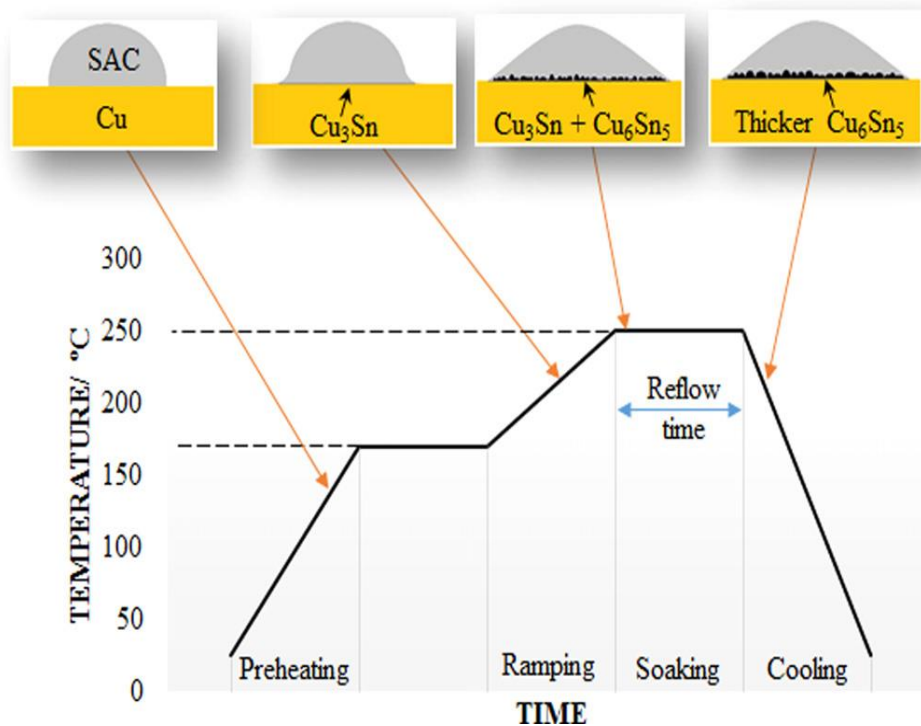


Figure 2.1: General soldering profile (Ting et al. 2015)

The cooling rate of solder alloys directly affects the microstructure of the Sn-Ag solders and also influences their mechanical behaviors. Hence, the effects of the applied cooling rate on microstructure and their properties have been studied. Shen et al. (2006) used 4 different cooling rates by changing the cooling method as a furnace, air, water and rapidly cooled. A fine distribution of spherical particles Ag_3Sn is observed at relatively fast cooling rates (24 K/s).

For comparison, Lee and Huang, (2015) performed an experiment of SAC305 samples in a different cooling methods which are cooled in water cooling, air cooling, and a furnace cooling. From the result, it is shown that water-cooled sample, with the highest cooling rate of 100°C/s , consisted small of particle-like Ag_3Sn phase in a eutectic network with no Cu_6Sn_5 phase observed. By contrast, the sample cooled in the air (cooling rate of 2.09°C/s) contained not only plate-like Ag_3Sn compound but also the rod-like Cu_6Sn_5 phase.

Finally, for sample cooled in the furnace (cooling rate of 0.008°C/s) presented a coarsened eutectic structure that consist of large plate-like Ag_3Sn and isolated rod-like Cu_6Sn_5 precipitates. The cooling rate will change the microstructure of IMC and also affect growth behavior of solder joint. In Figure 2.2, Deng et al. (2003) show the thermal profiles of Sn-3.5Ag/Cu joint during reflow and cooling in three different methods. Cooling in water, air, and furnace yielded approximate cooling rates of 106°C/sec , 5.4°C/sec , and 0.1°C/sec , respectively.

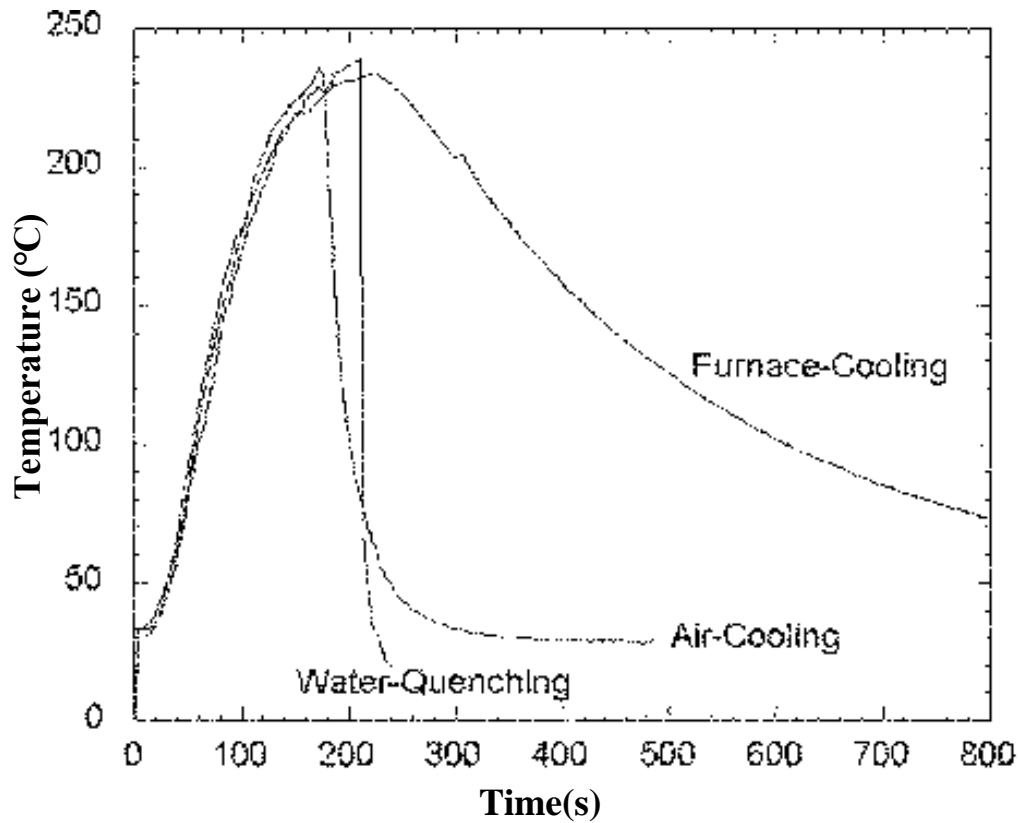


Figure 2.2: The thermal profiles of the Sn-3.5Ag/Cu joint during reflow and cooling in three different media (Deng et al. 2003)

2.4 Effect of reflow time

In order to understand the properties of SAC305 solder alloy by different temperature and time, it is necessary to investigate the phases that present on it. XRD characterization was used to analyse and identify the phases present in the SAC305 solder alloy. X-ray diffraction is a non-destructive analytical technique used for characterizing the crystalline materials. It provides information on crystal structure, phase, preferred crystal orientation of SAC305 solder alloys. To support the results, Field Emission Scanning Electron Microscope (FESEM) was used to determine the microstructure analysis.

Lee et al. (2013) studied the effect of soldering time on the phase present in SAC305. The growth of the IMC layer affected by the time and temperature of the soldering process. Figure 2.3 showed are sharp and intensive reflections of Cu_6Sn_5 . The smaller peak of the Cu is obviously visible, which increase reflow temperature. The intensity of the Cu_3Sn phase was lower than Cu_6Sn_5 because the longer time for cooling and higher temperature will obtain this phase.

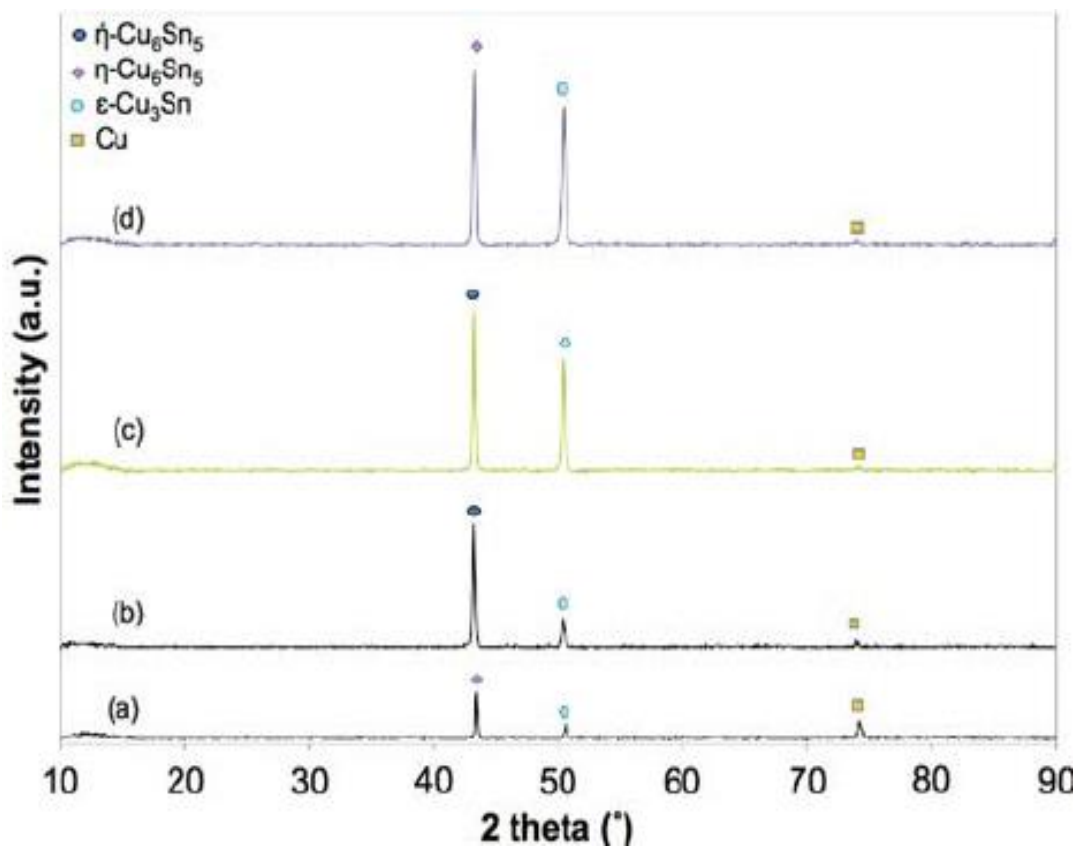


Figure 2.3: XRD analysis of SAC305/Cu at different reflow temperature (a) 230, (b) 240, (c) 250, and (d) 260°C for 30 s (Lee et al. 2013)

The thickness of the IMC layer depends on the reflow time and temperature. Therefore, the excessive growth of IMC result in defect and harmful to the reliability of solder joint. Figure 2.4a and Figure 2.4b showed the morphology of IMC layer at the interface with different reflow time.

It can be concluded that the lifetime of solder joint lifetime decrease rapidly with increase soldering temperature and time. The longer the reflow time, the coarser the IMC at the interface. Additionally, Tu et al. (1997) stated that thicker IMC layer will enlarge the probability of the failure of solder joints (a negative effect) because of the brittleness of the IMC. This explains why the reduction rate of the joint lifetime decrease as the IMC thickness increase.

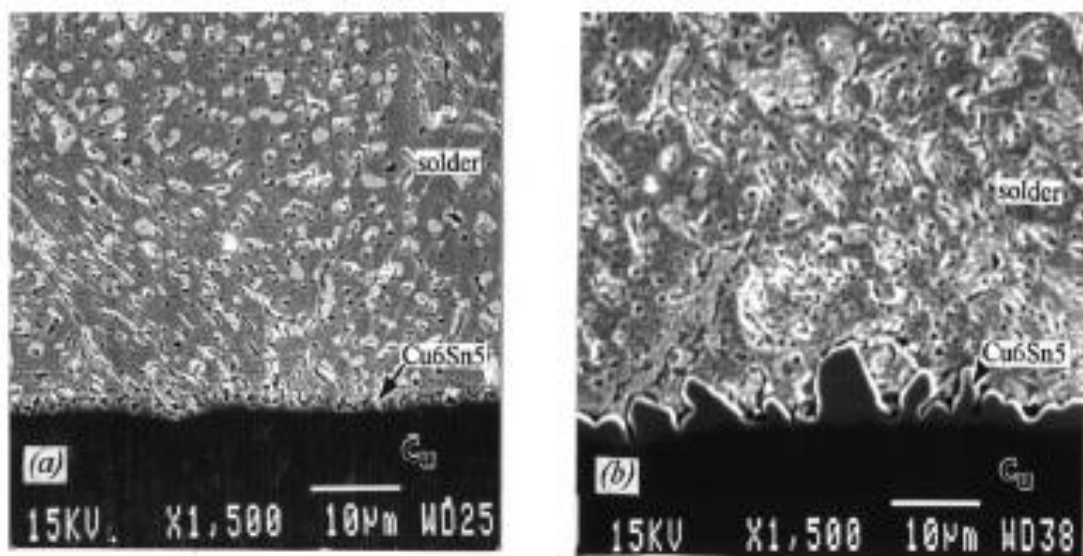


Figure 2.4: SEM micrographs of solder joints showing the IMC layers after (a) reflowing for 20 s and (b) reflowing for 600 s (Tu et al. 1997)

2.5 Effect of cooling rate

In Figure 2.5 showed the XRD pattern of SAC305 solder alloy at different cooling method. Wang et al. (2012) stated whether the cooling rate fast or slow there still shows that the constituent of SAC305 solder consists of β -Sn, Ag_3Sn , and Cu_6Sn_5 . In the solder reflow process, the critical importance stage of the cooling rate in the solidification shows that improper cooling rate coarsens the phases in the solder matrix.

The cooling method affects the phases present in solder. The higher the cooling rate, the finer the microstructure and also effect to the peak intensity. The effect of intensity depends on the diffraction angle. The lower the diffraction angle, the lower the intensity of the phases present. XRD analysis was evidence for the phase present in the SAC305 solder at different cooling rate.

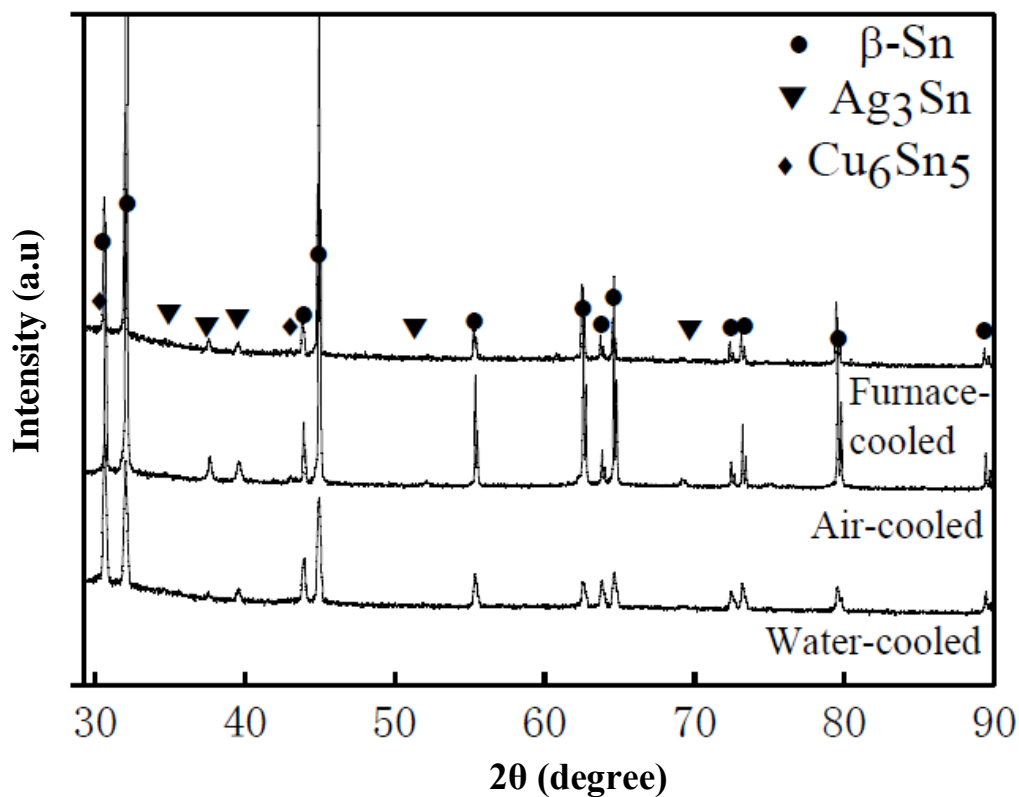


Figure 2.5: XRD pattern of SAC305 solder alloy at different cooling method (Wei & Wang 2012)

The different cooling method will affect the cooling rate of the solder. Cooling rate during solidification of SAC solders plays an important role in determining the morphological changes and microstructural evolution. Therefore, has a significant effect on the mechanical properties of the solder. There has been a study on the microstructural changes and morphological evolution of lead-free Sn-3.0Ag-0.5Cu solder subjected to various cooling rates in the range of 0.008°C/s to 100°C/s during the reflow soldering process (Lee and Huang, 2015).

Cooling rate of solder decreased as the time of cooling method and temperature longer and higher. The cooling rate and time during reflowed will influence the growth of IMCs layer. The Cu_6Sn_5 crystals will appear when anxious eutectic mixture of Sn and Ag_3Sn solidified inside the solder as the concentration of Sn drops. Due to the long-time above liquidus and the high peak temperature, more amount of copper was dissolved from the soldering pad. Different microstructures have different material and mechanical properties. The typical microstructures of Sn-Ag-Cu(SAC) lead-free solder alloys are made up of β -Sn grains, platelet-type Ag_3Sn , and scallop-type Cu_6Sn_5 .

Figure 2.6a shows typical microstructure of SAC solder alloy (Sun and Zhang, 2015). The needle-like of Ag_3Sn phases was coarsened for air cooled in Figure 2.6b and the size of β -Sn was smaller with tiny needle-like Ag_3Sn phase in Figure 2.6c for water cooled (Ji et al. 2014). The higher the cooling rate, the smaller the grain size of the microstructure. Due to the dispersion strengthening mechanism, smaller and uniform microstructure will give positive effects on the mechanical properties of the solder joint.

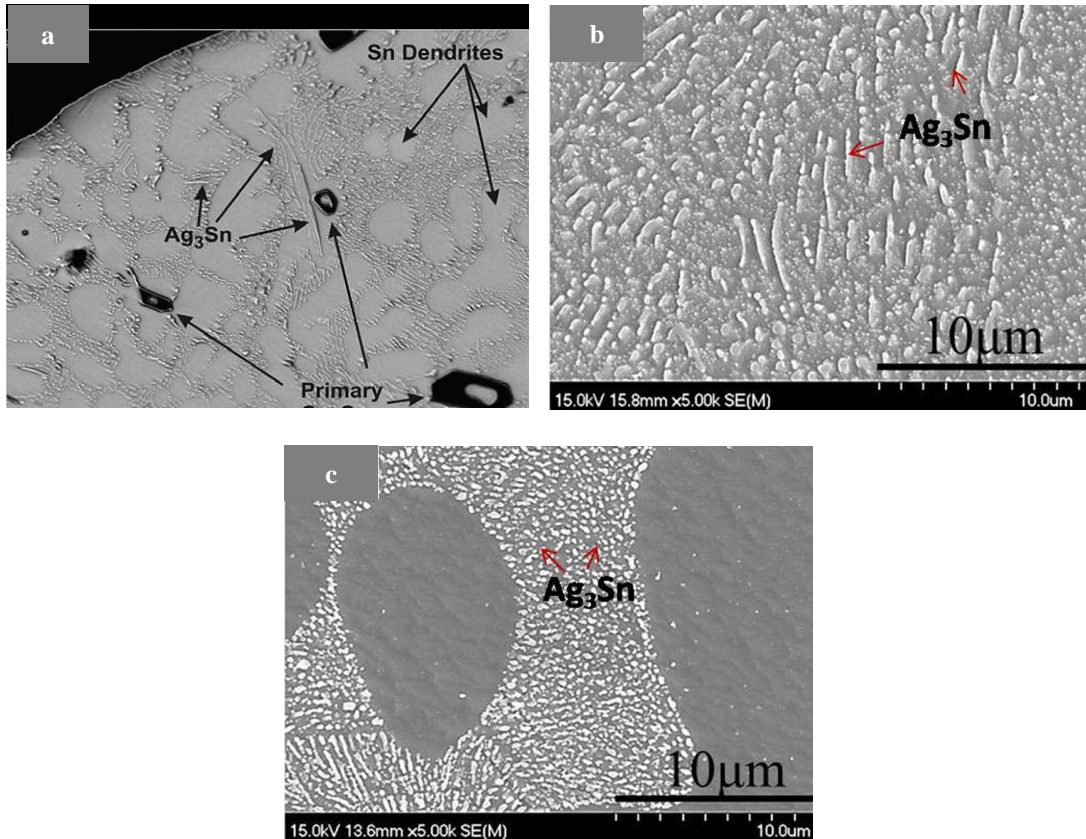


Figure 2.6: (a) The microstructure of SnAgCu solder (Sun and Zhang, 2015), (b) air cooled and (c) water cooled (Ji et al. 2014)

Figures 2.7 show the microstructure of solder joints samples cooled in water, air, and furnace for various hours, respectively. In Figure 2.7a there is only a single Cu_6Sn_5 layer at the interface in the aged samples for 120 h. As the aging time is prolonged to 240 h, a thin Cu_3Sn layer can form between Cu_6Sn_5 and Cu in Figure 2.7c and Figure 2.7e. Hu et al. (2016) stated that during reflow, more Cu atoms diffuse toward Cu_6Sn_5 to form Cu_3Sn phase within a sufficient time.

Hu et al. (2016) and Deng et al. (2003) conclude that higher reflow times contributed to a slightly thicker intermetallic layer. Size of the thickness of IMC increases from Figure 2.7(b,d, and f) as the time increases. According to the Figure 2.7e, there are some void forms in white circles within the Cu_3Sn layer with a long-term of solid-state reaction because of the brittle properties of IMCs that result in crack within the IMCs.

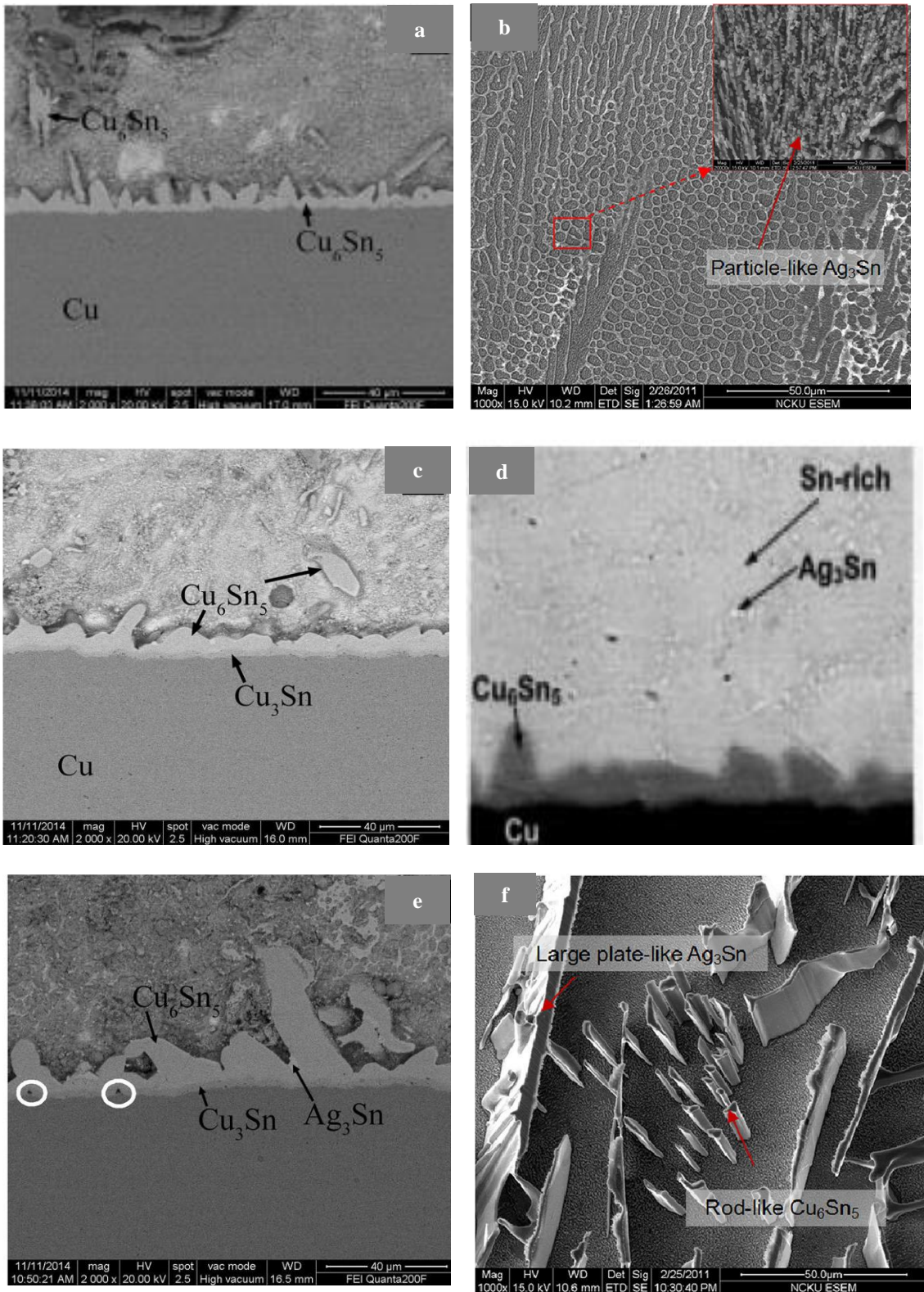


Figure 2.7: Microstructure of solder joints cooling in water, cooling in air cooling in a furnace for (a,c,e) Hu et al. (2016) and (b,d,f) (Deng et al. 2003),(Lee and Huang, 2015)

Yang and Zhang, (2015) investigated that different cooling methods will give different growth behavior of intermetallic compounds (IMC) in SAC305 solder joints, including the interfacial Cu_6Sn_5 layer and Ag_3Sn in the solder. In this study, three different type of cooling methods used which is quenched water, cooling in air and cooling in a furnace after reflow. In the reflow process, Sn atoms in the solder reacted with Cu substrate forming the interfacial IMC layer.

Figure 2.8 showed the image morphology of the IMC at the interface between the Cu substrate and solder after water quenching (Figure 2.8a), air cooling (Figure 2.8b), and furnace cooling (Figure 2.8c). From the figure, it can observe that different cooling rate have different IMC thickness. Figure 2.8d show that the highest IMC thickness was furnace cooling with $4.99 \mu\text{m}$ and the lowest with $1.92 \mu\text{m}$ for water quenching. The IMC thickness for air cooling was $2.33 \mu\text{m}$ and slightly more than water quenching. This indicated that the growth of Cu_6Sn_5 IMC layer was thicker because the time for growth in this cooling process was longer than quenched in water. This could happen because there was two mechanism of growth for interfacial Cu_6Sn_5 .

The earliest in order of mechanism is Cu atoms of the substrate react with molten Sn because there is a concentration gradient of Cu atoms between Cu_6Sn_5 grains with different radius. The second mechanism is formed by reaction with Sn at the $\text{Cu}_6\text{Sn}_5/\text{Sn}$ interface that indicates the growth of interfacial Cu_6Sn_5 is diffusion of Cu atoms from small Cu_6Sn_5 grains to large grains. In addition, no obvious Cu_6Sn_5 or Ag_3Sn IMC were detected in the specimen quenched in water as the cooling rate higher, which indicated that formation of IMC had limited time to grow.

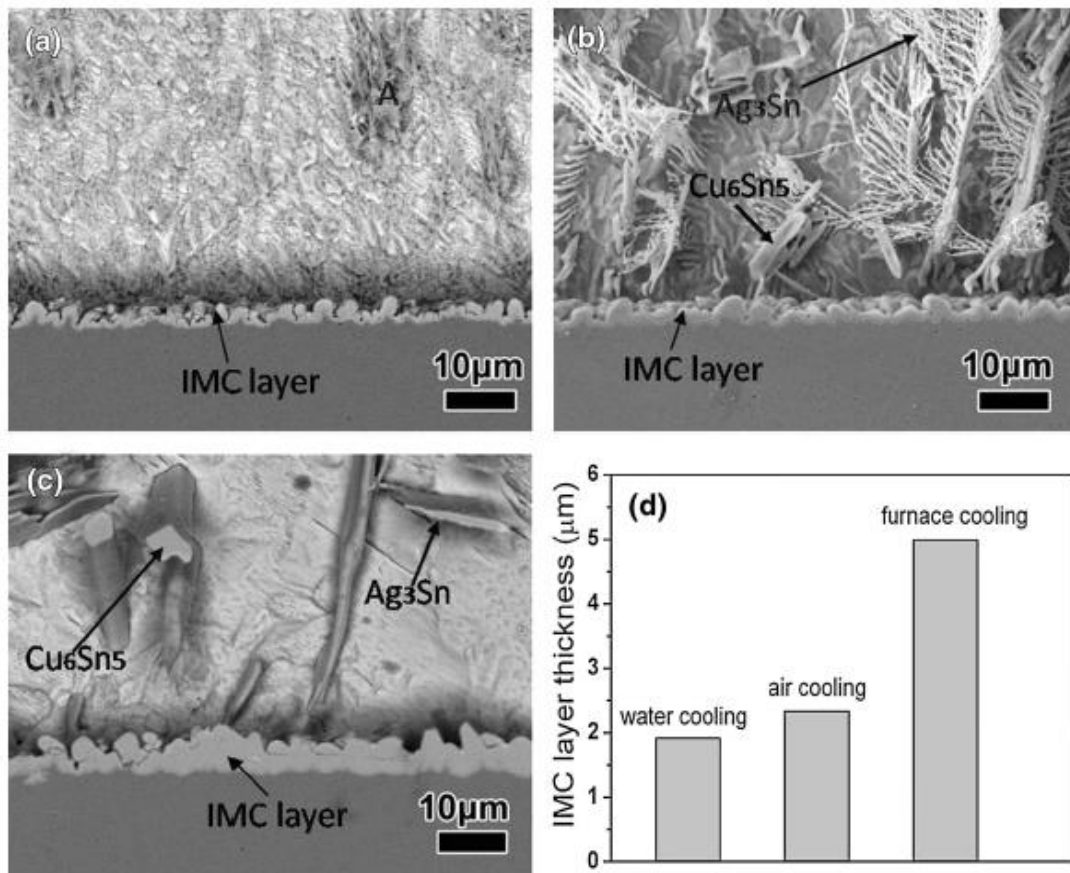


Figure 2.8: SEM images of SAC305 solder joints: (a) quenched in water, (b) cooled in air, (c) cooled in a furnace, (d) variation of the thickness of the Cu₆Sn₅ IMC layer (Yang and Zhang, 2015)

2.6 Corrosion characterization of SAC305 solders

Corrosion is defined as the destruction or deterioration of a material due to a chemical or an electrochemical reaction with its environment. It is of great importance to study the performance of the material to the corrosion behavior. There are several methods to determine the corrosion behavior such as Weight loss corrosion testing, Open Circuit Potential (OCP), Potentiodynamic polarization and Electrochemical Impedance Spectroscopy (EIS). The changes of structural and morphology of the SAC305 solder will influence the corrosion behavior.

A simplest test for measuring corrosion is the weight loss method. This method involves exposing a clean weighed piece of the metal or alloy to the corrosive environment for a specified time. After that, followed by cleaning process to remove corrosion products and weighing the piece to determine the loss of weight. The rate of corrosion (R) is calculated as:

$$R = kW / \rho At$$

where k is a constant, W is the weight loss of the metal in time t, A is the surface area of the metal exposed, and ρ is the density of the metal (in g/cm³).

Open circuit potential change as a function of time contains information of the interfacial structure and electron transfer kinetics on an electrode surface (Chen, 2008). Four different alloy with different composition were studied which are Sn-0.7Cu, Sn-3.5Ag, Sn-0.3Ag-0.7Cu and Sn3.5Ag-0.7Cu (composition in wt.%). The alloys were measured in 3.5 wt.% NaCl aqueous solution at 21°C. An OCP was measured immediately after sample was immersed in the electrolyte. From the result, it is shown that the corrosion resistance increases with increasing transition metal concentration. The highest OCP value obtained was Sn-3.5Ag and Sn-3.5Ag-0.7Cu alloy and the lowest observed for Sn (Martin et al. 2015).

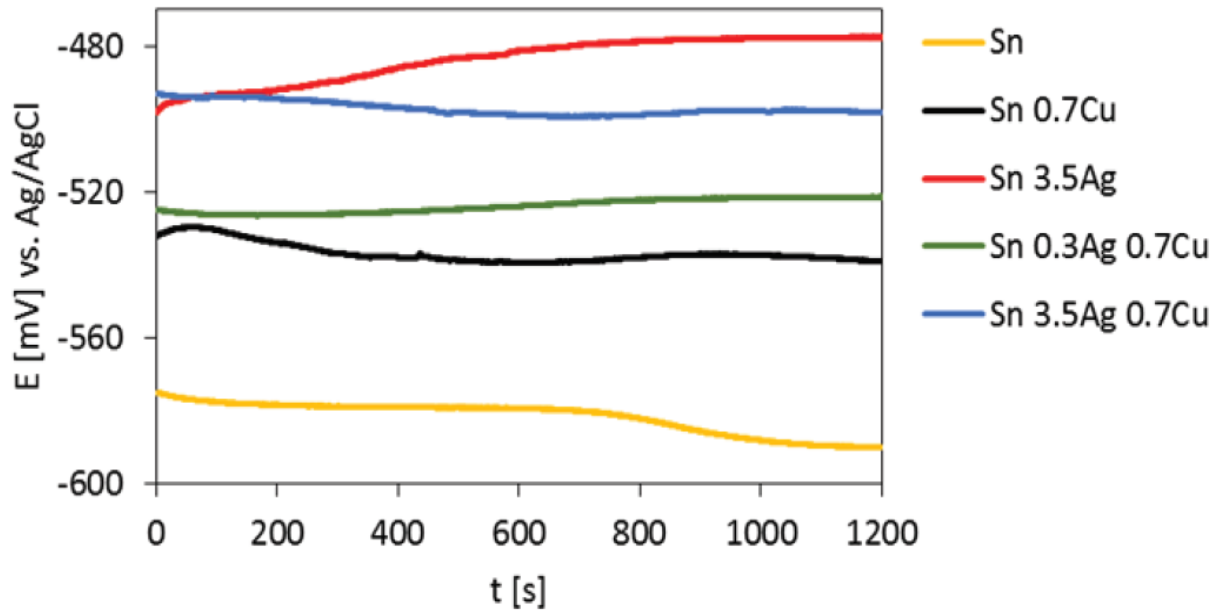


Figure 2.9: Open circuit potential of lead-free solders (Martin et al. 2015)

Potentiodynamic polarization methods used to determine the information regarding corrosion mechanisms, the corrosion rate of specific materials to corrosion in different cooling methods. It is also used to polarize the SAC305 and the mixed of corrosion products on the surface of SAC305 solder will present.

Basically, (i_{corr}) plays a more important role in evaluating the corrosion resistance. The corrosion potential (E_{corr}) reflects the tendency to corrode, while the corrosion current density (i_{corr}) shows the degree of corrosion. Several different parameters (open circuit potential, rupture potential, passivity range, pitting corrosion) can be derived from the same run. Different cooling method has different corrosion rate and behavior of SAC305 solder alloy.

Figure 2.10 shows the potentiodynamic polarization curves of SAC305 solder alloys with various cooling methods in 3.5 wt% NaCl solution. For commercial SAC305 solder, the anodic current density never exceeds $5 \mu\text{Acm}^{-2}$ and passivation start at -840

mV/SCE and extending to -420 mV/SCE. The passivation starts due to formation of Sn oxides, SnO and SnO₂.

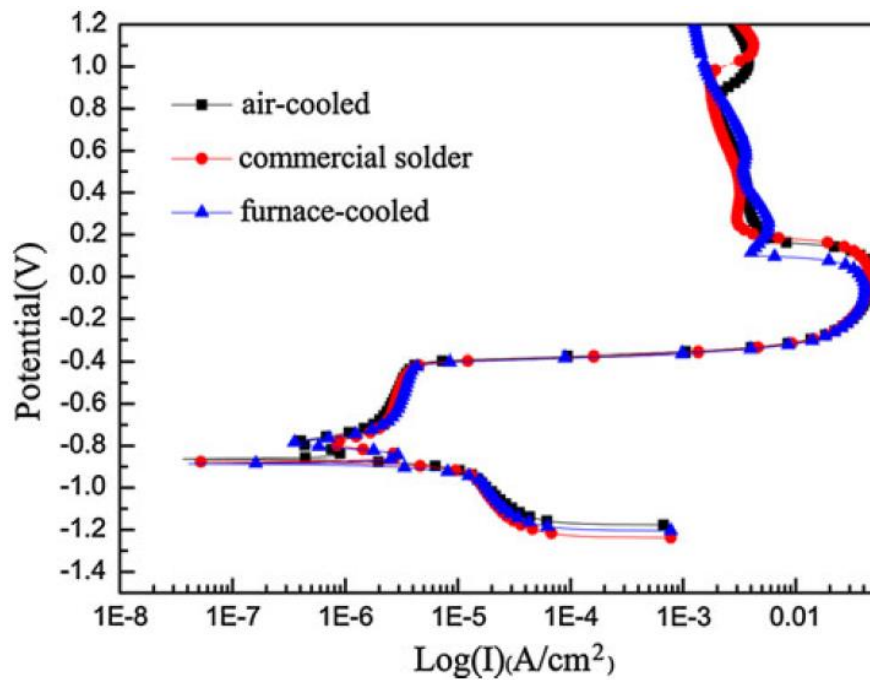


Figure 2.10: Potentiodynamic polarization curves of SAC305 solders at different cooling methods in 3.5 wt% NaCl solution (Wang et al. 2012)

Wang et al. (2012) stated the XRD analysis of corrosion product film in Figure 2.11 by anodic polarization at +500 mV /SCE for 1800 s in 3.5 wt% NaCl solution. Three phases detected were Sn, Ag₃Sn, and Sn₃O(OH)₂Cl₂. From the XRD analysis, the result showed all solder of different cooling method had same corrosion product, Sn₃O(OH)₂Cl₂ which was a complex oxide chloride hydroxide of Sn.

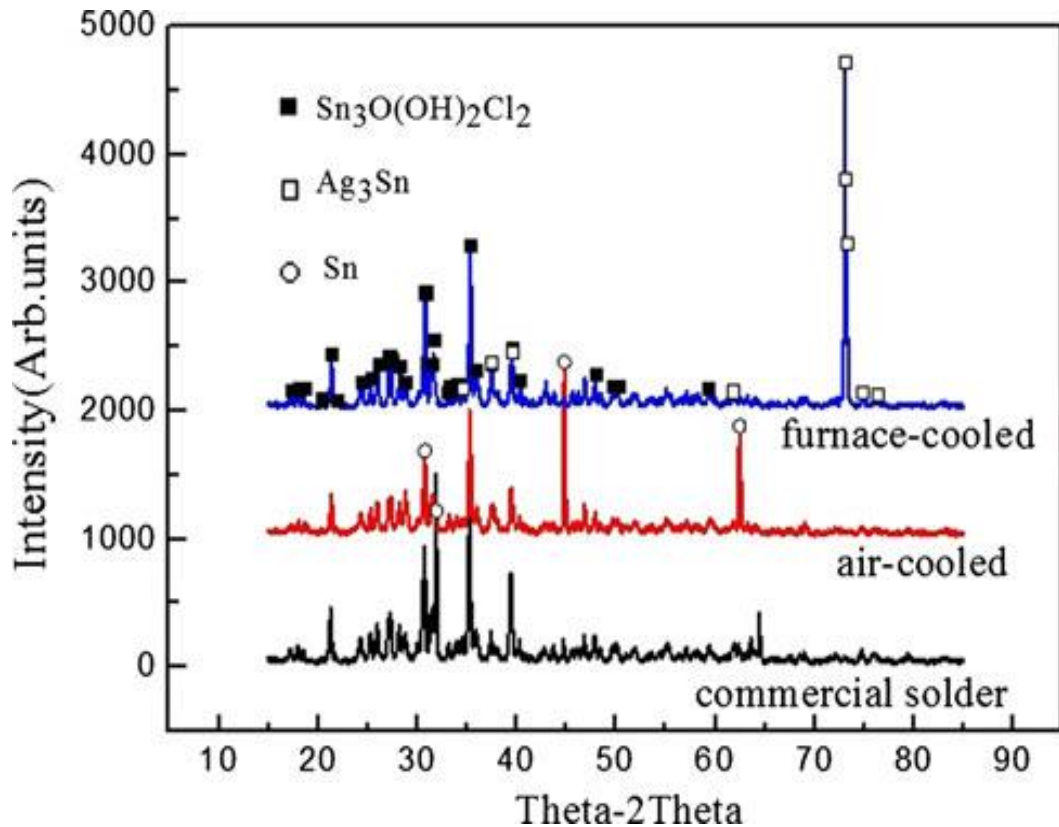


Figure 2.11: XRD pattern from corrosion products of SAC305 solders after anodic polarization at +500 Mv /SCE for 1800 s in 3.5% NaCl solution at 25 °C (Wang et al. 2012)

Fayeka et al. (2017) stated that potentiodynamic polarization test was conducted using A Gamry Potentiostat (Gamry instrument, Inc., USA). The electrochemical corrosion was investigated in 3.5 wt% NaCl solution.

Potentiodynamic polarization test was carried out in Figure 2.12 with a potential range of -1000V to +1000 mV versus the reference electrode at a scan rate of 1 mV/s. Corrosion potential and current density values were determined by Tafel plot method. From the graph, it can be seen that SAC305 has the largest passivation range with lowest critical current density indicating its highest corrosion resistance compared to SA and SAC305 solder alloy.

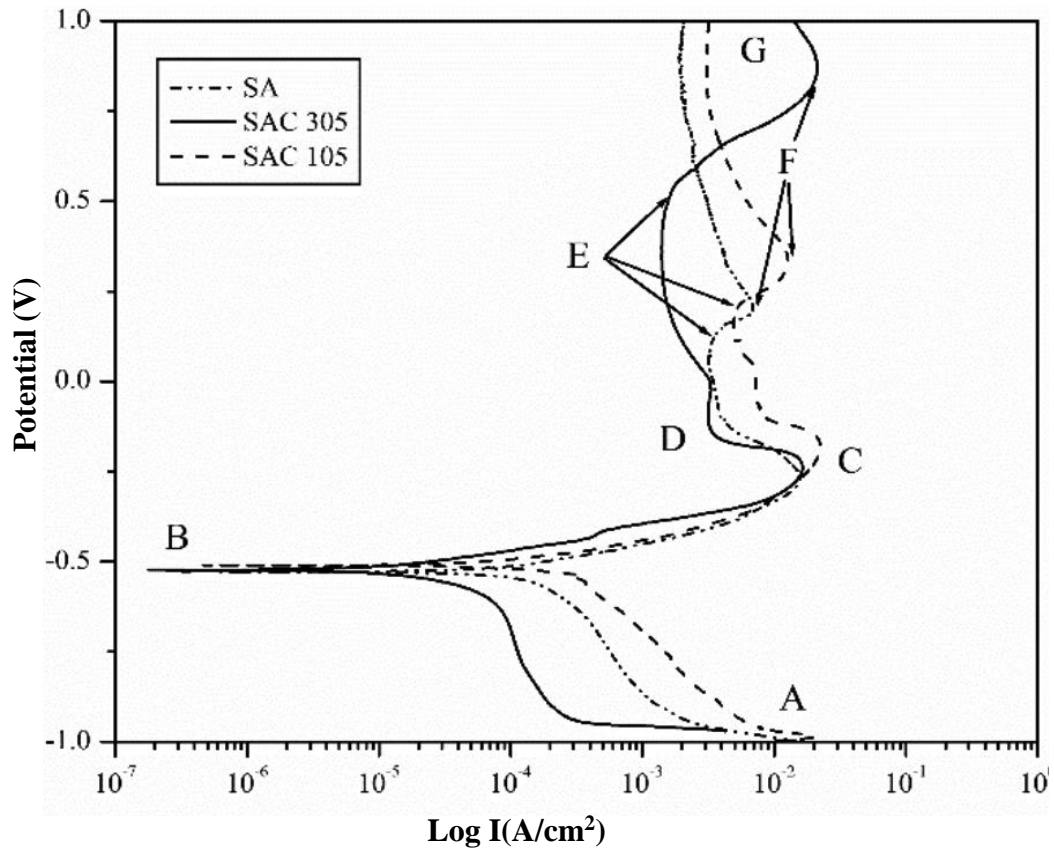
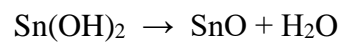
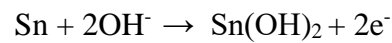
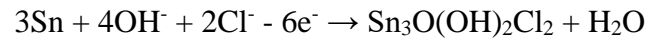


Figure 2.12: Potentiodynamic polarization curves of SA, SAC 305 and SAC 105 solder alloys in 3.5 wt% NaCl solution (Fayeka et al. 2017)

Fayeka et al. (2017) also stated in Figure 2.13, several phases are detected at surface which are $\text{Sn}_3\text{O}(\text{OH})_2\text{Cl}_2$, $\text{Sn}_3\text{O}(\text{OH})_2$, SnO_2 , SnO , Cu_6Sn_5 and Ag_3Sn . The formation of tin oxide may take place through the following reactions (Mohran et al 2009).



The corroded product on SAC105 and SAC305 confirmed to be $\text{Sn}_3\text{O}(\text{OH})_2\text{Cl}_2$. This might have formed according to the following reaction:



Based on the result, the formation of the oxides at the sample surface introduces the passivation that contributes to reducing the corrosion rate.

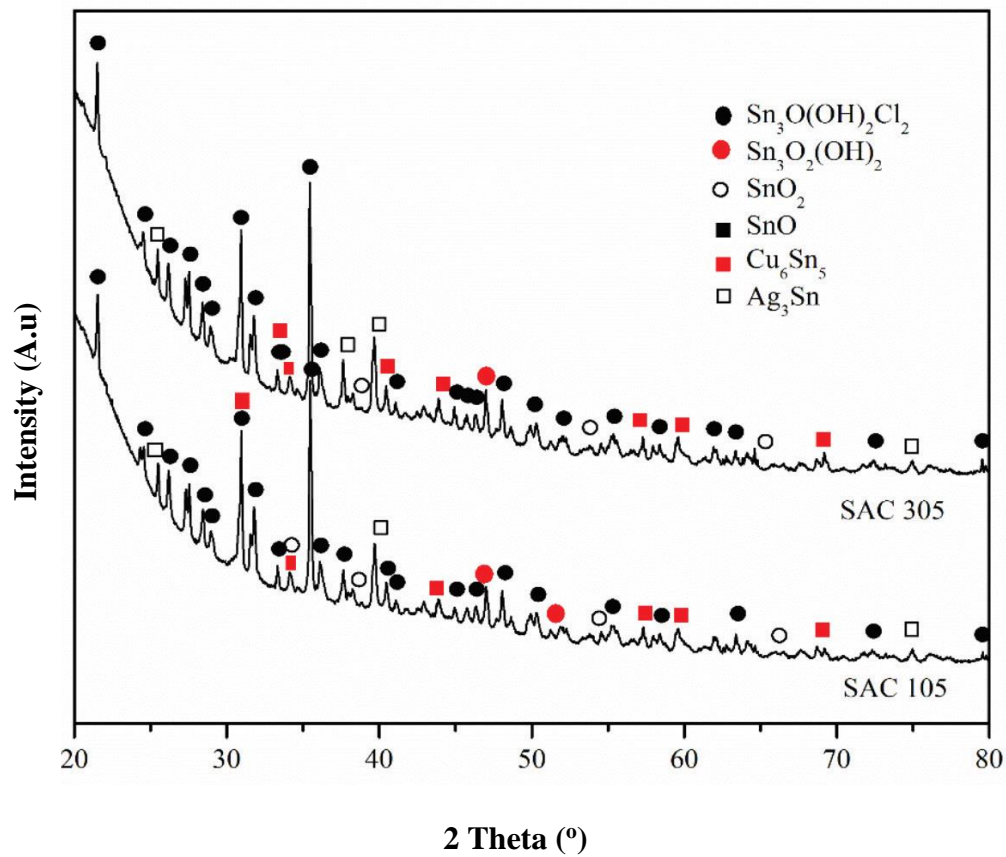


Figure 2.13: X-ray diffraction pattern of SAC105 and SAC305 after polarization (Fayeka et al. 2017)